

運輸省港湾技術研究所

(30th Anniversary Issue)

港湾技術研究所 報告

REPORT OF
THE PORT AND HARBOUR RESEARCH
INSTITUTE

MINISTRY OF TRANSPORT

VOL. 31 NO. 5 MAR. 1993

NAGASE, YOKOSUKA, JAPAN



港湾技術研究所報告 (REPORT OF P.H.R.I.)

第31巻 第5号 (Vol. 31, No. 5) 1993年 3月 (Mar. 1993)

目 次 (CONTENTS)

1. Estimation of Sliding Failure Probability of Present Breakwater for Probabilistic Design
..... Tomotsuka TAKAYAMA and Naota IKEDA ... 3
(確立設計に向けた現行防波堤の滑動確立の推定 高山知司・池田直太)
2. Experimental Study on Impulsive Pressures on Composite Breakwaters
..... Shigeo TAKAHASHI, Katsutoshi TANIMOTO and Ken'ichiro SHIMOSAKO ... 33
(混成防波堤に作用する衝撃碎波力に関する研究 高橋重雄・谷本勝利・下迫健一郎)
3. Beach Erosion in a Storm due to Infragravity Waves
..... Kazumasa KATOH and Shin-ichi YANAGISHIMA ... 73
(荒天時の長期周波によるバーム浸食 加藤一正・柳嶋慎一)
4. Water Exchange in Enclosed Coastal Seas Kazuo MURAKAMI ... 103
(閉鎖性内湾域の海水交換 村上和男)
5. Multiple Regression Wave Forecast Model Described in Physical Parameters
..... Chiaki GOTO, Hidenori SHIBAKI and Toshio AONO ... 135
(物理因子重回帰波浪予測モデル 後藤智明・柴木秀之・青野利夫)
6. Wave-induced Liquefaction in a Permeable Seabed
..... Kouki ZEN and Hiroyuki YAMAZAKI ... 155
(海底砂地盤の波浪による液状化 善 功企・山崎浩之)
7. Development of Design Method for Concrete Pavements on Reclaimed Ground
— Its Application to Tokyo International Airport —
..... Yoshitaka HACHIYA and Katsuhisa SATOH ... 193
(埋立地盤上におけるコンクリート舗装設計法の開発 — 東京国際空港への適用 —
..... 八谷好高・佐藤勝久)
8. Analysis of Liquefaction Induced Damage to Sheet Pile Quay Walls
..... Susumu IAI and Tomohiro KAMEOKA ... 221
(液状化による矢板式岸壁の地震時被害の数値解析 井合 進・亀岡知弘)

9. A Study on Durability of Concrete Exposed in Marine Environment for 20 Years
..... Tsutomu FUKUTE and Hidenori HAMADA ... 251
(海洋環境に20年間暴露されたコンクリートの耐久性に関する研究..... 福手 勤・濱田秀則)

10. Applications of a Ship Maneuvering Simulator to Port and Harbor Planning
..... Tadanobu HAYAFUJI, Yuichi KURODA, Kenji HAMADA and Koji SAKAI ... 273
〔操船シミュレーターの港湾計画への応用 早藤能伸・浜田賢二・黒田祐一・酒井浩二〕

11. Development of an Aquatic Walking Robot for Underwater Inspection
Hidetoshi TAKAHASHI, Mineo IWASAKI, Jyun'ichi AKIZONO,
..... Osamu ASAKURA, Shigeki SHIRAIWA and Katsuei NAKAGAWA ... 313
〔走行式水中調査ロボットの開発 (第二報)
..... 高橋英俊・岩崎峯夫・秋園純一・朝倉 修・白岩成樹・中川勝栄〕

12. Fluidity Characteristics of Muddy Slurry with Compressed Air in Horizontal Pipe
Yoshikuni OKAYAMA, Takeyuki FUJIMOTO,
Motokazu AYUGAI, Makoto SUZUKI and Yuuya FUKUMOTO ... 359
(水平管における空気混入軟泥の流動特性
..... 岡山義邦・藤本健幸・鮎貝基和・鈴木 誠・福本裕哉)

5. Multiple Regression Wave Forecast Models Described in Physical Parameters

Chiaki GOTO*
Hidenori SHIBAKI**
Toshio AONO***

Synopsis

The Multiple Regression wave forecast models described in physical parameters, named MRPH models, are developed. In the MRPH models, ocean waves are described by two representative waves: wind waves and swells. The propagation speed of each wave components assumed to be constant. From these assumptions, governing equations of the MRPH models are expressed as linear algebraic equations. Explanation variables are energy of wind waves and swells in each direction.

To verify the MRPH models, wave forecast was carried out for three ports in Japan. The MRPH models were confirmed to have a greater accuracy in forecasting than any other models. The MRPH models also solve the difficult problem of eliminating the delay time of predicted values to observed ones which often appears at the initial stage of wave growth in the conventional multiple regression models. The MRPH models maintain a high level of accuracy even in the case of long term wave forecasting. Furthermore, the MRPH models are able to predict items which can not be predicted by the existing statistical models such as wave period, direction, and the component value of wind waves and swells.

Key Words: Wave forecast model, multiple regression models, physical factors, wave hindcast models.

* Chief, Ocean Energy Utilization Laboratory, Hydraulic Engineering Division.

** Research Trainee, (ECOH Co., Ltd.), Ocean Energy Utilization Laboratory, Hydraulic Engineering Division.

*** Ocean Energy Utilization Laboratory, (National Institute Post Doctoral Fellow), Hydraulic Engineering Division.

5. 物理因子重回帰波浪予測モデル

後 藤 智 明*・柴 木 秀 之**・青 野 利 夫***

要 旨

港湾建設の施工管理から船舶の航行、海洋性レクリエーションに至る幅広い海洋活動における安全性の確保には、的確な波浪予測情報の提供が不可欠である。従来より、波浪予測を目的として用いられてきた手法として波浪推算モデル、統計モデルがある。しかしながら、波浪推算モデルでは、推算結果をそのまま予測値とすることに波浪予測精度上の問題があり、また、重回帰波浪予測モデルでは、予測波高の立ち上がりの遅れや長期予測に対する予測精度の低下といった実用化を考える上で多くの課題が残されていた。

本研究では、これらの問題を克服するための新たな手法として、波浪推算モデルと統計モデルのそれぞれの長所を組み合わせた物理因子重回帰モデルを提案し、その予測理論を述べるとともに、現地へ適用した結果と予測精度に関する考察を行った。得られた結論は以下の通りである。

- ①物理因子重回帰モデルは、本来なら微分方程式で記述される波浪の発達、伝播、減衰を、代数方程式に書き換え、係数を回帰的に算定し、これを波浪予測式としている。
- ②物理因子重回帰モデルによる出力緒元は、有義波高、有義波周期のみならず、波向、風波とうねりそれぞれの相当有義波高、相当有波周期、成分波波向である。
- ③予測モデルAの係数は、期間が長いほど次第に平均的な値になる傾向を有する。また、モデルBの短期予測式の係数は観測波浪に強く依存する傾向を持つが、長期予測では依存度は低下する。
- ④物理因子重回帰モデルは、従来の手法に比べ良好な予測精度を有し、重回帰モデルの大きな欠点であった予測値の時間遅れの問題を解決している。また、長期予測についても、重回帰モデルのように著しく予測精度が低下する問題もない。

キーワード：波浪予測モデル、重回帰モデル、物理因子、波浪推算モデル

* 水工部 海洋エネルギー利用研究室長

** 水工部 海洋エネルギー利用研究室 研修生（㈱エコー）

*** 水工部 海洋エネルギー利用研究室（科学技術特別研究員）

Contents

Synopsis	135
1. Introduction	139
2. Theory of wave forecasting	139
2.1 Assumptions	139
2.2 Model A	141
2.2.1 Forecasting theory for significant wave height	141
2.2.2 Forecasting theory for significant wave period	143
2.3 Model B	144
2.4 Consideration of sheltering effects	145
3. Application of MRPH models	145
3.1 Locations of wave forecasting	145
3.2 Duration for multiple regression analysis	145
3.3 Forecasting of marine surface winds	145
3.4 Identification of regression coefficients	146
3.5 Forecasting result for significant wave	147
3.5.1 Predicted significant wave	147
3.5.2 Predicted components both wind waves and swells	150
4. Accuracy of wave forecasting	150
5. Conclusion	152

1. Introduction

Reliable wave information is indispensable for maintaining safe ocean activities such as the construction of maritime structures, the navigation of ships, marine recreation, etc.. Especially, in managements of port and harbor construction works, it is important to develop a reliable wave forecasting system.

Recently, numerical wave hindcast models^{1),2),3)} based on an energy equilibrium equation have been used for the wave forecasting. However, such wave hindcast models have some problems concerning accuracy. A major object of wave hindcast models are the hindcasting of very high wave height ranging 4.0 m – 15.0 m which is encountered in a typhoon or monsoon. But the low wave height is most important in wave forecasting as this pertains to the critical height (0.5 m – 1.5 m) for maritime works. Both the verification of equations and the determination of any parameters are carried out on such high wave height conditions. Furthermore, results of wind hindcasting are inaccurate in lower wave height condition so wave hindcasting is still not satisfactory.

As alternative to wave hindcast models, statistical models (for example, multiple regression model^{4),5),6)}) have been proposed. An advantage to using statistical models is that equations are expressed as multiple regression forms so that the wave height in present time, the wind velocity and the pressure are members of variables, thereby allowing the calculation to be readily carried out without any special knowledge. However, owing to the strong reliance on observed wave height in statistical models, predicted wave height is subject to delay. Furthermore, the accuracy of wave forecasting decreases with long term wave forecasting. There are many difficulties for practical use.

In this study, a new model which departs from conventional methods is proposed: Multiple Regression wave forecast models described in Physical parameters (MRPH). The MRPH models hold advantages over both the wave hindcast model and the statistical model.

The proposed MRPH models consist of two different models, Model A and Model B. Model A describes each process of wave growth, wave propagation and wave decay, and is a kind of wave hindcast model. The main difference between Model A and conventional wave hindcast model is that the governing equations of Model A are expressed by a set of algebraic equations, while the wave hindcast model is expressed by a set of partial differential equations. As the governing equations of the model are expressed by a set of algebraic equations, the coefficients contained in the model can be identified by the comparison between calculated wave energy and observed wave energy explicitly. Furthermore, the forecasting results are more accurate.

Model B is formulated on the basis of Model A, but is modified to decrease the prediction error by considering the difference in the predicted and observed wave energy every forecasting hour and in the changing rate of wave energy.

As compared with multiple regression models, the coefficients of both Model A and B are able to be understood physically. And output constituent of these models is not only significant wave height and period, but also representative wave direction predicted by evaluated wave energy distribution on each wave direction, and the component value of both wind waves and swells.

2. Theory of wave forecasting

2.1 Assumptions

In order to formulate multiple regression models described in physical parameters,

the following assumptions are applied to wave growth, wave propagation and wave decay.

The growth of wave height is described with $1/2$ power law for nondimensional significant wave height and fetch, and wave period with $1/3$ power law⁷⁾ for nondimensional significant wave period and fetch. As shown in Fig. 1, wave rays propagate radially in sixteen directions centered to the location of wave forecasting. Wave growth and decay go on independently on each ray.

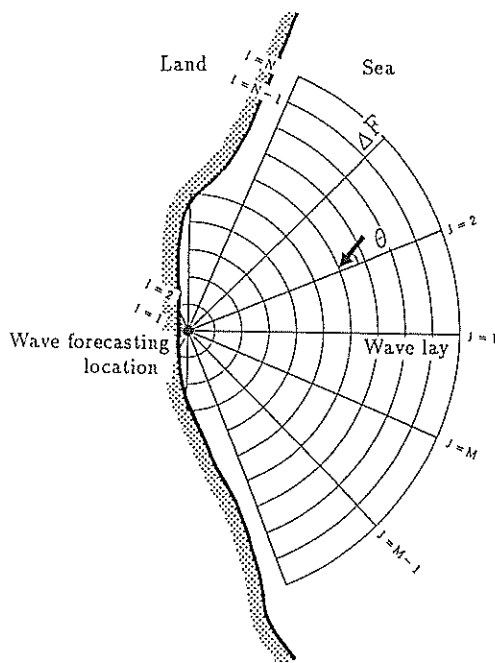


Fig. 1 Schematic diagram of the location of wave forecasting and wave rays radially

Essentially, wave propagation speed varies depending on wave growth, but in these models, waves are described by two wave components: wind waves and swells. The wave period and the propagation speed for each wave component are assumed to be constant. The propagation of wind waves and swells is described by each characteristic line as shown in Fig. 2. In these models, from the consideration of the wind prediction with six hour intervals, the optimum period of wind waves and swells is chosen. Specifically, significant wave period of wind waves is 6.9s (5.9s: mean wave period) based on the assumption that wave propagates 200 km per 6 hours. As for the swells, significant wave period is 13.8s (11.9s: mean wave period) and wave propagates 200 km per 6 hours.

Furthermore, wave decay is treated similar to Bretshneider's equation⁸⁾. Namely, in regions of favorable wind, decay of wind waves does not occur until the wind energy equilibrium is attained. For wave going away from wind field or a wave coming into the adverse wind field, the energy of swells decays in inverse proportion to propagation distance, and the period of swells increases in proportion to propagation distance.

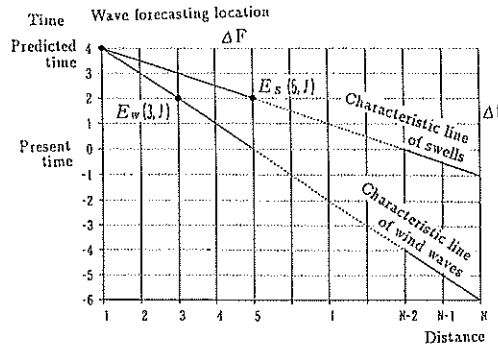


Fig. 2 The characteristic lines of propagation for wind waves and swells in any direction

2.2 Model A

2.2.1 Forecasting theory for significant wave height

From above assumptions, by using $1/2$ power law for nondimensional wave height and fetch, equation of wind wave development is described as follows:

$$\left[\frac{gH_{1/3}}{U^2} \right] = a' \left[\frac{gF}{U^2} \right]^{1/2} \quad (1)$$

where $H_{1/3}$ is a significant wave height, U the wind velocity at a height of 10 m above sea surface, F a fetch, g the gravity acceleration, respectively.

Then, energy equation of wind waves is

$$\left[\frac{g^2 \varepsilon}{U^4} \right] = a' \left[\frac{gF}{U^2} \right] \quad (2)$$

where ε is energy of wind waves. Equation (2) is the governing equation for wind wave development in this study. And energy distribution in each direction of wind waves is assumed to always maintain a similar profile, thus,

$$\varepsilon = \int_0^{2\pi} E(\theta) d\theta, \quad E(\theta) = \varepsilon \lambda(\theta), \quad (3)$$

where $E(\theta)$ is energy component of wind waves which propagates from the direction of θ , $\lambda(\theta)$ is a directional distribution function defined as:

$$\lambda(\theta) = \begin{cases} \lambda_0 \cos^4 \theta & (-\pi/2 \leq \theta \leq \pi/2) \\ 0 & (\theta < -\pi/2, \theta > \pi/2), \end{cases} \quad (4)$$

where λ_0 is a normalized coefficient that satisfies the following relation

$$\int_0^{2\pi} \lambda(\theta) d\theta = 1. \quad (5)$$

From Eq. (2), (3), (4) and (5), the energy of wind waves in each direction is

$$E(\theta) = \varepsilon \lambda(\theta) = AFU^2 \lambda(\theta), \quad A = a/g. \quad (6)$$

In an arbitrary wave direction, wind energy $U^2 \lambda(\theta)$ on characteristic line of wind waves is described as shown in Fig. 3. In a certain wave direction J , considers the case of wind waves

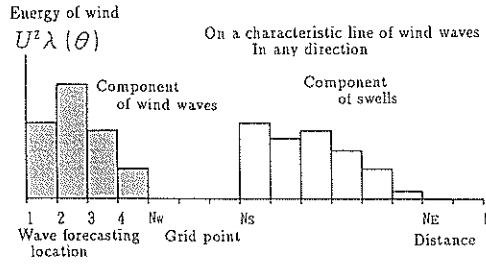


Fig. 3 Schematic representation of wind energies distribution on the characteristic line on wind waves propagation

growing between $I = 1$ and $I = N_w$ within the grid points from $I = 1$ to $I = N$. From Eq. (6), energy of wind waves is noted as follows.

In direction J , energy of wind waves at $I = N_w$ is $E(N_w, J) = 0$, thus $E(N_w - 1, J)$ at $I = N_w - 1$ is

$$E(N_w - 1, J) = A \Delta F U(N_w - 1, J)^2 \lambda(N_w - 1, J), \quad (7)$$

where ΔF is the distance between adjacent grid points. Similarly, energy of wind waves at $I = N_w - 2$ is

$$E(N_w - 2, J) = A(F_T + \Delta F)U(N_w - 2, J)^2 \lambda(N_w - 2, J), \quad (8)$$

where F_T is equivalent fetch so that energy of wind waves at $I = N_w - 1$ is $E(N_w - 1, J)$ under the condition that component of wind energy is $U(N_w - 2, J)^2 \lambda(N_w - 2, J)$, and written as follo

$$F_T = \frac{E(N_w - 1, J)}{AU(N_w - 2, J)^2 \lambda(N_w - 2, J)}. \quad (9)$$

By substituting Eq. (9) into Eq. (8), Eq. (8) is rewritten as:

$$\begin{aligned} E(N_w - 2, J) &= E(N_w - 1, J) + A \Delta F U(N_w - 2, J)^2 \lambda(N_w - 2, J) \\ &= A \Delta F U(N_w - 1, J)^2 \lambda(N_w - 1, J) + A \Delta F U(N_w - 2, J)^2 \lambda(N_w - 2, J). \end{aligned} \quad (10)$$

Similar arrangements are carried out from $I = N$ to $I = 1$, and energy of wind waves in direction J is expressed as:

$$[N_w(J)] = A \Delta F \sum_{I=1}^{N_w-1} U(I, J)^2 \lambda(I, J) \quad (11)$$

and the wave energy in all directions is as follows:

$$[\epsilon]_w = \sum_{J=1}^{16} [N_w(J)] = B_w \sum_{J=1}^{16} \sum_{I=1}^{N_w-1} U(I, J)^2 \lambda(I, J), \quad (12)$$

where B_w is the coefficient nearly equal to $A \Delta F$, and is defined as results of regression analysis between calculated wave energy and observed wave energy.

By considering the case that wind waves are transformed to swells and propagate between $I = N_s$ and $I = N_e$, as shown in Fig. 4, initial energy of swells is equivalent to that of wind waves at $I = N_s$, so the following equation is obtained,

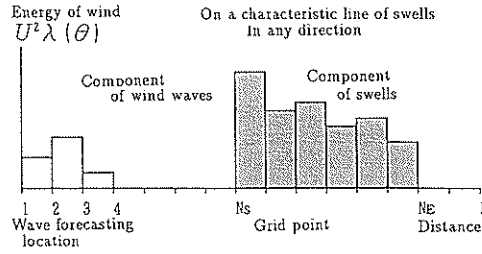


Fig. 4 Schematic representation of wind energies distribution on the characteristic line of swells propagation

$$E_w(N_s, J) = A' \Delta F \sum_{I=N_s}^{N_E} U(I, J)^2 \lambda(I, J). \quad (13)$$

Swells are assumed to decay in inverse proportion to the propagation distance, so energy of swells at $I = 1$ is

$$[E_s(J)] = A' \Delta F \frac{E_w(N_s, J)}{(N_s - 1) \Delta F}, \quad (14)$$

where A' is the same kind of coefficient to A in Eq. (6). According, total energy of swells in all directions is summed up as follows:

$$[\varepsilon_s] = B_s \sum_{J=1}^{16} [E_s(J)], \quad (15)$$

where B_s is the coefficient nearly equal to $A' \Delta F$, and is defined the same as B_w in Eq. (12).

From Eq. (12) to (15), total energy of wind waves and swells at $I = 1$ is

$$[\varepsilon_f] = [\varepsilon_w] + [\varepsilon_s] = B_w \sum_{J=1}^{16} [E_w(J)] + B_s \sum_{J=1}^{16} [E_s(J)], \quad (16)$$

where $[\varepsilon_f]$ is the predicted wave energy. Conversion of predicted wave energy to the significant wave height is carried out by Eq. (17).

$$H_{1/3} = 3.83 \sqrt{[\varepsilon_f]}. \quad (17)$$

2.2.2 Forecasting theory for significant wave period

By using 1/3 power law for nondimensional significant wave period and fetch, the growth of wind waves in period is expressed as:

$$\left[\frac{gT_{1/3}}{U} \right] = c \left[\frac{gF}{U^2} \right]^{1/3} \quad (18)$$

By raising both members of Eq. (18) to 3th power, the following equation is obtained.

$$\left[\frac{g^3 \tau}{U^3} \right] = \left[\frac{gT_{1/3}}{U} \right]^3 = c \left[\frac{gF}{U^2} \right]^3 \quad (19)$$

where τ is a significant wave period to the 3th power, and is defined as a characteristic period in this study.

Similar to 2.2.1, the directional distribution function $\lambda(\theta)$, as Eq. (4), of the characteristic period is defined. From this, Eq. (19) is able to be rearranged, so characteristic period in each direction is

$$T(\theta) = \tau\lambda(\theta) = CFU\lambda(\theta), \quad C = c/g^2 \quad (20)$$

In a similar manner as with the wave height, characteristic period of wind waves in all directions is described as follows:

$$[\tau]_w = D_w \sum_J [D_w(J)] = D_w \sum_J \sum_{I=1}^{N_w} U(I, J) \lambda(I, J), \quad (21)$$

where D_w is the coefficient nearly equal to $C\Delta F$, and determined as the result of regression analysis similar to the case of wave height.

Period of swells is assumed to increase in proportion to the propagation distance, so characteristic period of swells in all directions is,

$$[\tau]_s = D_s \sum_{J=1}^{16} [T_s(J)] = D_s \sum_{J=1}^{16} \sum_{I=N_s}^{N_E} U(I, J) \lambda(I, J), \quad (22)$$

where D_s is the coefficient that is defined the same as D_w in Eq. (21).

From Eqs. (21) and (22), characteristic period at the location of wave forecasting is described as:

$$[\tau]_f = \frac{D_w \sum_{J=1}^{16} [E_w(J)] [T_w(J)] + D_s \sum_{J=1}^{16} [E_s(J)] [T_s(J)]}{B_w \sum_{J=1}^{16} [E_w(J)] + B_s \sum_{J=1}^{16} [E_s(J)]} \quad (23)$$

where predicted characteristic period $[\tau]_f$ is defined as a weighed average value of wave energy in each direction. Conversion from the characteristic period to the significant wave period is carried out by Eq. (24).

$$T_{1/3} = [\tau]^{1/3} \quad (24)$$

2.3 Model B

Model B is formulated on the basis of Model A. However, Model B has a function to minimize the difference between calculated and observed wave energy at every calculating stage. The wave prediction error E_r , brought by Model A is not Gaussian, but may be caused by any other physical factors. The factors related to the wave prediction error are the difference between calculated and observed wave energy at present time, and the changing rate of calculated wave energies.

From above consideration, the wave prediction error is described as follows:

$$\begin{aligned} E_r = & C_1 [\varepsilon]_{Mb} - a \sum_{J=1}^{16} [E_{wb}(J)] - b \sum_{J=1}^{16} [E_{sb}(J)] \\ & + C_2 \left\{ \sum_{J=1}^{16} [E_w(J)] - \sum_{J=1}^{16} [E_{wb}(J)] \right\} \\ & + C_3 \left\{ \sum_{J=1}^{16} [E_s(J)] - \sum_{J=1}^{16} [E_{sb}(J)] \right\} \\ & + E'_r, \end{aligned} \quad (25)$$

where $E_w(J)$ and $E_s(J)$ are calculated energies of wind waves and swells at the forecasting time, respectively, and $E_{wb}(J)$ and $E_{sb}(J)$ are calculated energies at the present time. The symbol $[e]_{Mb}$ is observed wave energy at the present time. By assuming error as written in Eq. (25), the equation of Model B is formulated as follows:

$$[\varepsilon] = B_M[e]_{Mb} + B_W \sum_{j=1}^{16} [E_w(J)] + B_S \sum_{j=1}^{16} [E_s(J)] \\ + B_{wb} \sum_{j=1}^{16} [E_{wb}(J)] + B_{sb} \sum_{j=1}^{16} [E_{sb}(J)], \quad (26)$$

where five coefficients in Eq. (26) are defined by the regression analysis similar to Model A. As for characteristic period of Model B, the following equation is described.

$$[\tau]_f = D_M[\tau]_{Mb} \\ + \frac{D_W \sum_{j=1}^{16} [E_w(J)] [T_w(J)] + D_S \sum_{j=1}^{16} [E_s(J)] [T_s(J)]}{B_W \sum_{j=1}^{16} [E_w(J)] + B_S \sum_{j=1}^{16} [E_s(J)]} \\ + \frac{D_{wb} \sum_{j=1}^{16} [E_{wb}(J)] [T_{wb}(J)] + D_{sb} \sum_{j=1}^{16} [E_{sb}(J)] [T_{sb}(J)]}{B_{wb} \sum_{j=1}^{16} [E_{wb}(J)] + B_{sb} \sum_{j=1}^{16} [E_{sb}(J)]}. \quad (27)$$

2.4 Consideration of sheltering effects

In case of adapting the MRP models to coastal locations, the consideration of sheltering effects by lands is important. In this study, since the coefficients in each direction are equivalent, sheltering effects are considered in the following way.

Correctional coefficients for each calculated energy of wind waves ($E_w(J)$) and swells ($E_s(J)$) are introduced and adopted according to sheltering rate by lands and capes. For the wave rays toward land shorter than 100 km, correctional coefficients are also carried out by multiplying the energy by the coefficients in proportion to distance.

3. Application of MRP models

3.1 Locations of wave forecasting

Long-term wave observation data is required for the application of the MRP models at the location of wave forecasting. In this study, three ports are selected for the wave forecasting: the port of Hitachinaka, the port of Mutsu-ogawara facing the Pacific Ocean, and the port of Fukaura facing the Japan Sea.

3.2 Duration and Schedule of multiple regression analysis

The forecast analysis is scheduled from February 1th to 28th, from May 1th to 31th, from August 1th to 31th, from November 1th to 30th in 1983, and from January 17th to February 28th, from April 17th to May 16th, from August 1th to 31th, and from September 27th to October 24th in 1989. These time periods incorporate the four seasons, and total duration is 252 days (about 8 months).

3.3 Forecasting of marine surface winds

In MRP models, marine surface wind at a height of 10 m is the necessary input data for the calculation of wave energy. In this study, calculation process of marine surface wind is as follows:

1. Evaluate atmospheric pressure distribution on grid points from isobalic line by using the typhoon wind model.
2. Evaluate wind by using the hybrid model combined with the gradient wind model and the typhoon wind model.
3. Convert evaluated wind into marine surface wind by the atmospheric boundary layer model⁹⁾.

3.4 Identification of regression coefficients

In order to determine the regression coefficients in the MRPH models, multiple regression analysis is carried out at the port of Hitachinaka, the port of Mutsu-ogawara, and the port of Fukaura. Identification of regression coefficients is performed for each of the eleven different time period, namely, one for each month, in February, May, August, November of 1983, January to February, May, August, from September to October of 1989, and for four months in 1983 and in 1989, and for eight months in all.

Figure 5 shows eleven series of regression coefficients for wave height of wind waves and swells which are calculated by 12 hours wave forecasting Model A, at the port of Hitachinaka. In case that the duration of identifying the coefficients is one month, obtained coefficients differ from each duration remarkably. In the case of four months, obtained coefficients are close to the average value over the case of one month. Furthermore, in the case of eight months, obtained coefficients show approximately the average value over the case of four months in 1983 and in 1989. Therefore, the regression coefficients are gradually approaching the average values as the duration of analysis are longer. Because the coefficients for eight months are approximately the same as those for four months, it is expected that the difference of coefficients between the case of eight months and a case of longer duration would only be slight.

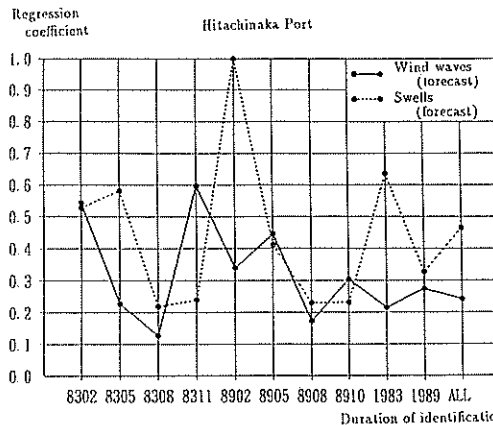


Fig. 5 Relation between regression coefficients and the duration of identification for significant wave height forecasting using Model A

Figure 6 shows the regression coefficients for wave height by Model B. Wave forecasting term using Model B is 6 hours, 12 hours, 24 hours, 36 hours, 48 hours, 72 hours (3 days), 120 hours (5 days), 168 hours (one week) and regression coefficients are identified for the duration of eight months. As in Fig. 6, the value of the coefficient related to observed significant wave height at the present time shows high contribution (0.6 – 0.8) in the short term wave forecasting. Namely, the value from 60% to 80% of the predicted wave

Multiple Regression Wave Forecast Models Described in Physical Parameters

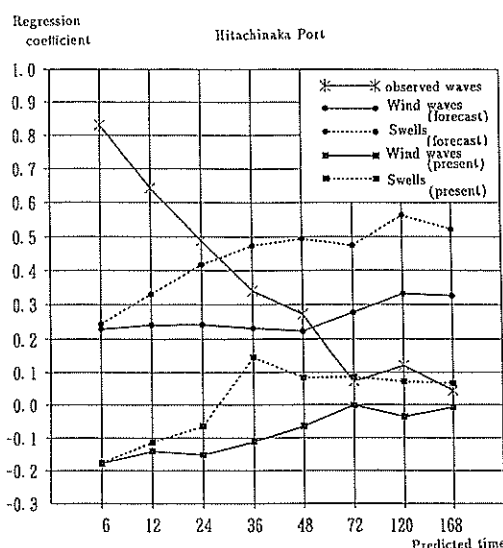


Fig. 6 Relation between regression coefficients and forecasting time for significant wave height forecasting using Model B

height is related to observed wave height at the present time. The coefficients, which are related to calculated wave energy of wind waves and swells at the prediction time, are positive. In contrast, the coefficients, which are related to the present time, are nearly equal to zero or negative. Furthermore, as the forecasting term becomes longer, there is a tendency for coefficients which were related to observed wave height at the present time to decrease, and for coefficients which were related to other variables to increase. This means that the predicted results strongly depend on observed waves in the short term wave forecasting. On the other hand, in the long term wave forecasting, the dependence on observed waves is weak and the dependence on the other explanation variables is strong. To make wave forecasting over a long term, such as after 120 hours or 168 hours, regression coefficients tend to gradually approach Model A.

3.5 Forecasting result for significant wave

3.5.1 Predicted significant wave

Forecasting of significant wave height and period is carried out over a period of eight months, in which the coefficients in equations of Model A and B are identified by regression analysis.

Figure 7 shows the comparison of predicted significant wave with observed one for 12 hours wave forecasting using Model A at the port of Hitachinaka in February of 1983. **Figure 8** shows the predicted significant wave for 12 hours wave forecasting using Model B, and **Fig. 9** shows 168 hours wave forecasting (long term wave forecasting), at same location and same duration in **Fig. 7**. These figures also show the predicted wave direction.

As in **Fig. 7**, the difference between predicted wave height and observed one is noticed near the peak during stormy wave conditions, but predicted wave height agrees approximately with observed one in the duration of both stormy waves and calm waves. As for the wave period, the predicted result is not in agreement with the observed one, but for a long term trend, the predicted result falls within acceptable engineering limits. As in **Fig. 8**, the

Hitachinaka Port

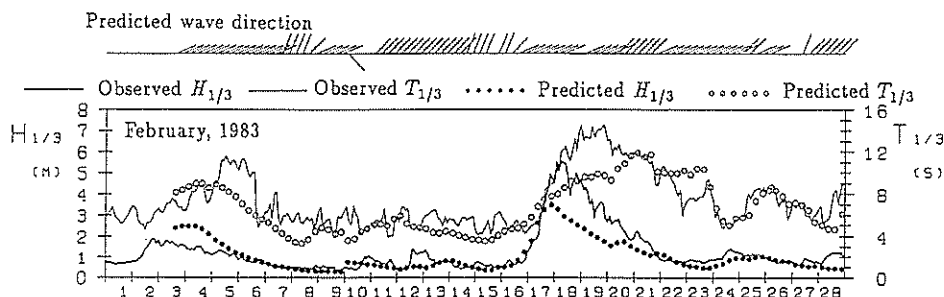


Fig. 7 Wave forecasting results and observed wave data at the port of Hitachinaka using Model A (12 hours wave forecasting)

Hitachinaka Port

After 12 hours

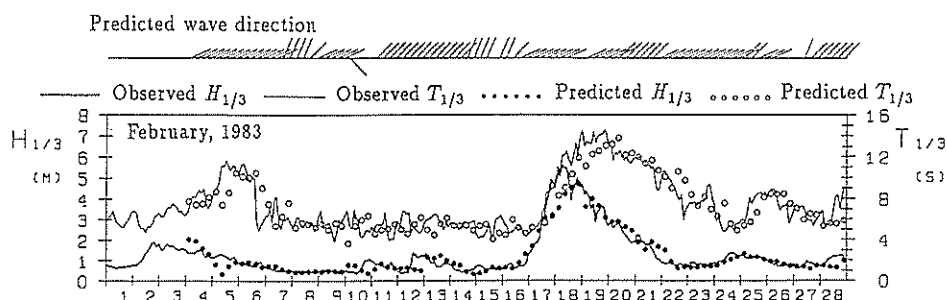


Fig. 8 Wave forecasting results and observed wave data at the port of Hitachinaka using Model B (12 hours wave forecasting)

Hitachinaka Port

After 168 hours

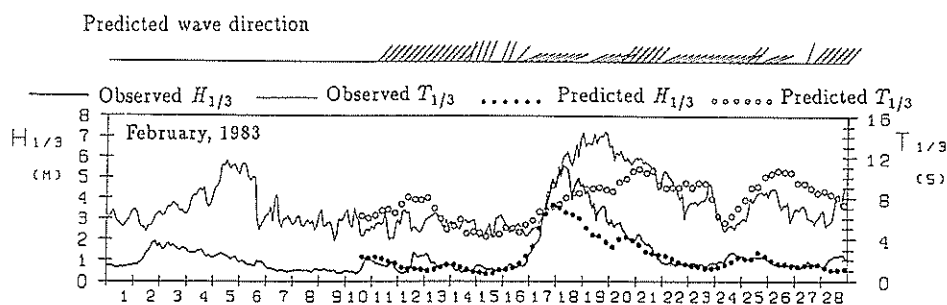


Fig. 9 Long term wave forecasting results and observed wave data at the port of Hitachinaka using Model B (168 hours wave forecasting)

predicted waves for 12 hours wave forecasting using Model B are in good agreement with the observed ones. As in Fig. 9, the predicted wave for 168 hours wave forecasting using Model B are similar to those in Fig. 7. Namely, the predicted waves using Model B tend to approach those using Model A as the wave forecasting term is longer.

Figure 10 shows the example of the 12 hours wave forecasting using conventional multiple regression model at the port of Mutsu-ogawara. In this figure, from the comparison of predicted significant wave height with that which was observed, delay time appears in the predicted wave height at the initial stage of stormy wave condition from 20th to 21st May, which is equal to wave forecasting term. On the other hand, as shown from Fig. 7 to Fig. 9, the predicted wave height using the MRP models agrees approximately with the trend of observed wave height.

Figures 11 and 12 show the comparison of predicted significant wave with observed significant wave for 12 hours wave forecasting using Model B, at the port of Mutsu-ogawara and the port of Fukaura, respectively. As in Fig. 11, the predicted waves agree with the observed ones at the port of Mutsu-ogawara. However, at the port of Fukaura, in Fig. 12, the degree of agreement with predicted waves and observed ones is not sufficient. In case of the port of Fukaura, wave forecasting is conducted during winter when stormy waves prevail on the Japan Sea. The wave component is mostly occupied wind wave components, and are affected considerably by the local wind fields

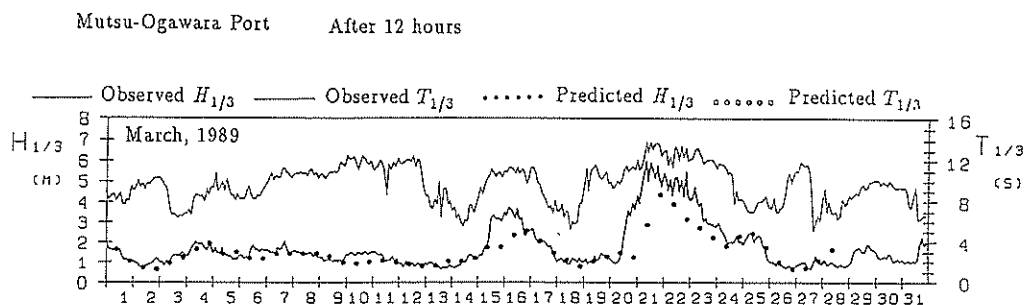


Fig. 10 Wave forecasting results and observed wave at the port of Mutsu-Ogawara using conventional multiple regression model (12 hours wave forecasting)

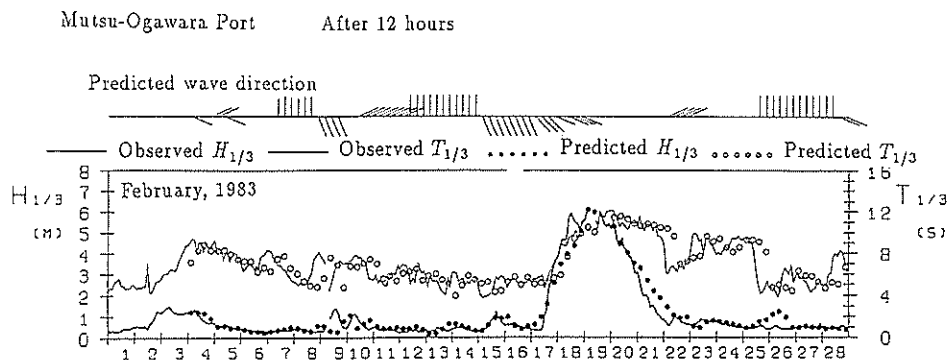


Fig. 11 Wave forecasting results and observed wave at the port of Mutsu-Ogawara using Model B (12 hours wave forecasting)

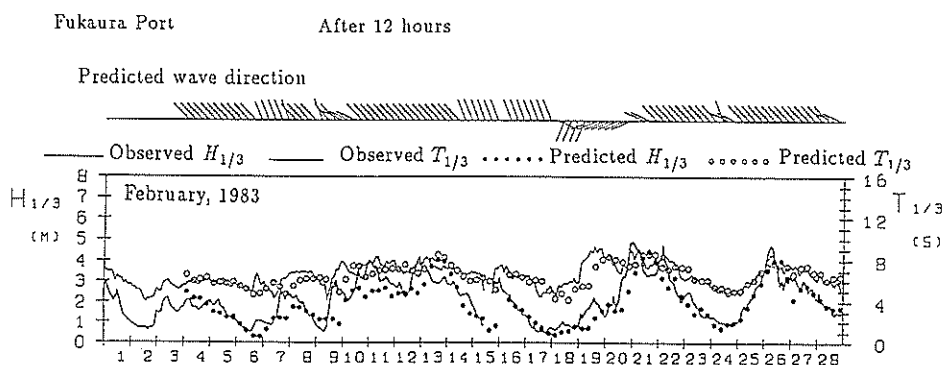


Fig. 12 Wave forecasting results and observed wave at the port of Fukaura using Model B (12 hours wave forecasting)

near the location of wave forecasting. Therefore, for the improvement of the wave forecasting accuracy at any location facing the Japan Sea, it is necessary to improve the hindcasting method of stormy wind attacking locally and periodically.

3.5.2 Predicted components both wind waves and swells

Figure 13 shows the evaluated significant wave height and period of wind waves and swells, respectively, with wave direction of each component for 12 hours wave forecasting using Model B. The location and the duration at Fig. 13 is same as in Fig. 8. There are no methods to sort wind waves from swells in observed wave data, so a quantitative comparison is not possible. However, by considering the topography around the port and characteristics of wind waves and swells, it is presumed that each time series of wave height, period and wave direction indicates interesting physical tendencies. The direction of compounded wave agrees with that of wind wave component during wave growth. While during wave decay and calm waves, the direction of compounded wave agrees with that of swell component. Judging from the equivalent wave height, wind wave component is highly occupied in the duration of maximum growing wave, on February 17th. On the other hand, swell component is highly occupied in the duration of wave decaying, on 20th to 21th, February. Also each predicted component of equivalent wave period shows that swell components are mostly longer than those of wind waves for about one month shown in the figure, and that the period of wind wave component approaches that of swell component only at the time of occurring maximum wave height in this duration.

4. Accuracy of wave forecasting

The fitting rate of wave forecasting on wave height is defined as a probability that the predicted result is included in a permissible error range of ± 0.3 m within the range of wave height between 0.0 m and 1.0 m, or $\pm 30\%$ of observed wave height greater than 1.0 m. In the case of wave period, the fitting rate is defined as the portion of $\pm 30\%$ error range to observed value all over the range.

Figure 14 shows the fitting rates evaluated from eight kinds of wave predicted results using Model A and B at three ports: the port of Hitachinaka, the port of Mutsu-Ogawara and the port of Fukaura. As in Fig. 14, the fitting rates show a tendency to decrease with the longer term wave forecasting, from 6 hours to 168 hours. However, the fitting rates in the case of 168 hours wave forecasting using Model B approach the same

Multiple Regression Wave Forecast Models Described in Physical Parameters

Hitachinaka

Predicted wave direction

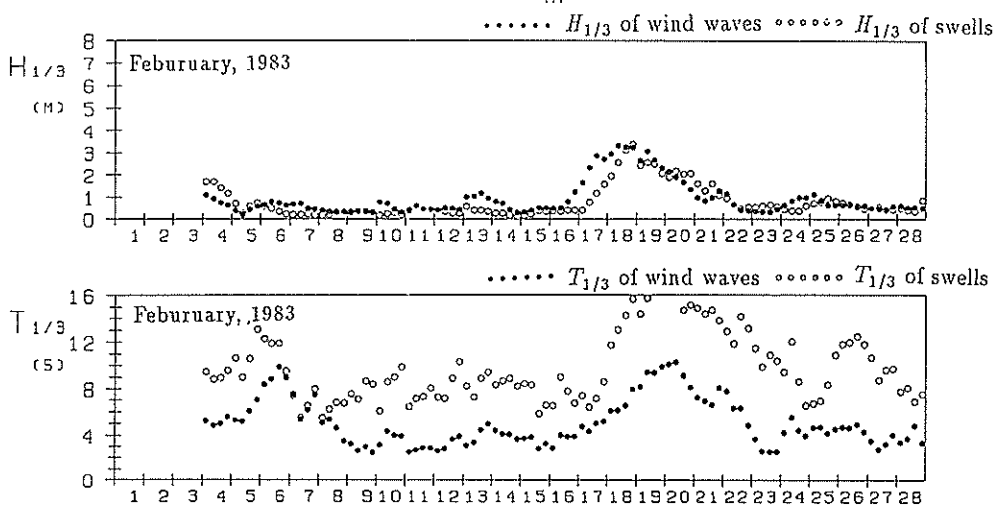
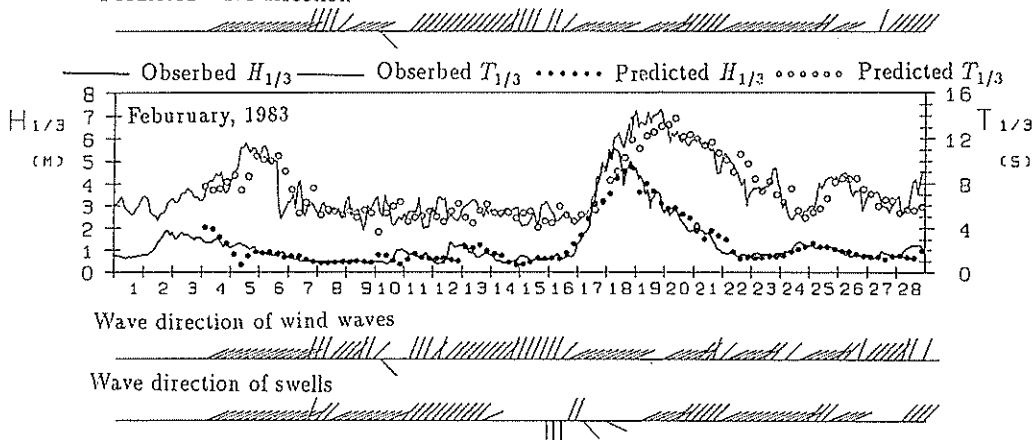


Fig. 13 Characteristics of wind waves and swells at the port of Hitachinaka using Model B

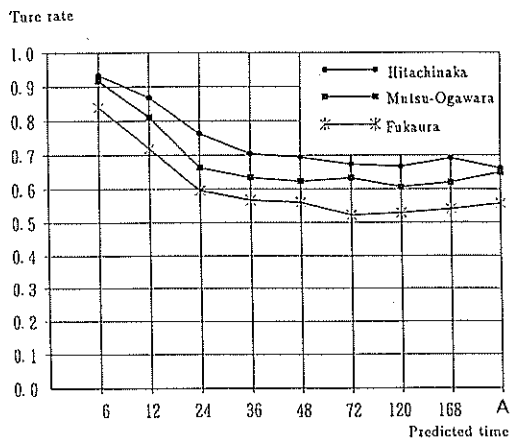


Fig. 14 The fitting rate of significant wave height and period using the MRP models (Model A and B)

level of Model A.

As stated in 3.4, this tendency is able to explain that predicted values depended weakly on observed waves, and that the equations of Model B approach those of Model A with the longer forecasting term.

Therefore, the accuracy of long term wave forecasting using Model B tends to approach that of Model A, and if the forecasting accuracy of Model A is enhanced, then the accuracy of long term wave forecasting would be improved correspondently.

5. Conclusion

In this study, Multiple Regression models described in Physical parameters, named MRPH models, are newly developed. These models include advantageous points of both wave hindcast model and statistical model. The results of this study may be summarized as follows.

① In the MRPH models, ocean waves are described by two representative waves: wind waves and swells, and the propagation velocity of each wave component is assumed to be constant. From these assumptions, governing equations of the MRPH models are expressed as algebraic equations, though wave growth, wave propagation and wave decay are essentially described as partial differential equations. The coefficients of algebraic equations can be obtained by regression analysis to minimize the error between calculated wave energy and observed one.

② Explanation variables in the MRPH models are energy of wind waves and swells in each direction. Predicted factors are not only significant wave height and period but wave direction, and the component of value both wind waves and swells, which have not been predicted by existing statistical model.

③ Parameter fitting of the wave forecasting equations is carried out to the three ports: the Port of Hitachinaka, the Port of Mutsu-Ogawara and the Port of Fukaura. The verification of the characteristic of regression coefficients is also carried out to the same ports. From this verification, the coefficients in the equation of Model A are modified with each duration of identification, but these values approach the average value with longer duration. The coefficients in the equation of Model B for short term forecasting show remarkable dependence on observed wave. As compared with this, the coefficients for long term wave forecasting decrease with longer forecasting term, and show a lower dependence on observed wave.

④ The MRPH models show greater accuracy of forecasting than the existing wave forecasting models, and solve the difficult problem of removing delay time during the initial stage of the waves growth. The MRPH models don't decrease the forecasting accuracy even in the case of long term wave forecasting. The MRPH models are expected to hold the dominant positions in wave forecasting in the near future.

(Received on August 31, 1992)

References

- 1) WILSON, B.W.: Numerical prediction of ocean waves in the North Atlantic for December, Deut. Hydgr., Vol. 18, pp. 114-130, 1965.
- 2) ISOZAKI, I AND T. UJI: Numerical Model of Marine Surface Winds and Its application the Prediction of Ocean Wind Waves, Papers in Met. and Geo, Vol. 25, No. 3, Sep. 1974.
- 3) YAMAGUCHI, M. AND Y. TSUCHIYA: Wave Prediction Methods in Limited Wind Fields,

- Pro. 26th Conf. Coastal Eng., JSCE, pp. 96–100, 1979. (in Japanese)
- 4) SUDA, K AND A. YUZAWA: Study on Wait Matrix of Seabase at Open Sea based on wave forecast. Proc. of JSCE, No. 339, pp. 177–185, 1983. (in Japanese)
 - 5) KOBUNE, K, N. HASHIMOTO, K. KAMEYAMA, M. KUDAKA: Applicability of Wave Forecasting Using Multiple Regression Methods, Proc. 34th Con. Coastal Eng., JSCE, pp. 167–171, 1987. (in Japanese)
 - 6) KOMAGUCHI, T, N. SHINDO, N. KAWAI AND K. KIMURA: Applications of Wave Forecasting Methods in Managements of Construction Works, Proc. 38th Conf. Coastal Eng., JSCE, pp. 961–965, 1991.
 - 7) GOTO, C, K. SUETSUGU AND K. KOBUNE: Investigation of the Wind Stress and Wave Growth Formulas, Proc. 38th Con. Coastal Eng., JSCE, pp. 170–174, 1990. (in Japanese)
 - 8) BRETSCHNEIDER, C.L.: Decay of Wind Generated Waves to ocean Swell by Significant Wave Method, Fundamental of Ocean Engineering, 8, Ocean Industry, 1968.
 - 9) SHIBAKI, H. AND C. GOTO: Dependence of Surface Wind on Inland Sea for Wind Driven Length and Land Topography, Proc. 40th Coastal Eng., JSCE, 1992. (in Japanese)

List of Symbols

A	: a/g a coefficient which relates to growth oh wind waves
A'	: a coefficient which relates to growth of swells
a	: squared on a'
a'	: a coefficients of $1/2$ power law
B_M	: a coefficient which relates to observed wave energy at the present time
B_S	: a coefficient which relates to calculated energy of swells at the forced time
B_{sb}	: a coefficient which relates to calculated energy of swells at the present time
B_W	: a coefficient which relates to calculated energy of wind waves at the forecast time
B_{wb}	: a coefficient which relates to calculated energy of wind waves at the present time
C	: c/g^2
c	: value of raised c' to 3th power
c'	: coefficient of $1/3$ power law
D_M	: a coefficient which relates to observed wave period at the present time
D_S	: a coefficient which related tob e calculated period of swells at the forecast time
D_{sb}	: a coefficient which related to e calculated period of swells at the forecast time
D_W	: a coefficient which related to be calculated period of wind waves at the forecast time
D_{wb}	: a coefficient which related to be calculated period of wind waves at the present time
E_r	: prediction error of model A
E'_r	: prediction error of model B
$[E_s(J)]$: calculated energy of swells in J direction at forecast time
$[E_{sb}(J)]$: calculated energy of swells in J direction at present time
$[E_w(J)]$: calculated energy of wind waves in J direction at forecast time
$[E_{wb}(J)]$: calculated energy of wind waves in J direction at present time
$E_w(N_w, J)$: initial energy of swells in J direction at N_w

$E(\theta)$: energy of wind waves in each direction
F	: fetch
F_T	: equivalent fetch
g	: gravity acceralation
$H_{1/3}$: significant wave height
U	: marine surface wind velocity
$T_{1/3}$: significant wave period
$[T_w(J)]$: characteristic period of wind waves in J direction at forecast time
$[T_{wb}(J)]$: characteristic period of wind waves in J direction at present time
$[T_s(J)]$: characteristic period of swells in J direction at forecast time
$[T_{sb}(J)]$: characteristic period of swells in J direction at present time
$T(\theta)$: characteristic period of wind waves in each direction
ε	: energy of wind waves
$[\varepsilon]_f$: total energy of wind waves and swells at forecast time
$[\varepsilon]_{Mb}$: energy of observed wave at present time
$[\varepsilon]_{Ms}$: total energy of swells in all directions at forecast time
$[\varepsilon]_w$: total energy of wind waves in all directions at forecast time
θ	: wave direction